Journal of Materials Chemistry C

ROYAL SOCIETY OF CHEMISTRY

PAPER

Cite this: J. Mater. Chem. C, 2021, 9, 15990

Synthesis and characterization of solution processable, high electron affinity molecular dopants†

Jan Saska,[a] Nikolay E. Shevchenko,[a] Goktug Gonel,[b] Zaira I. Bedolla-Valdez,[b] Rachel M. Talbot,[b] Adam J. Moulé *[b] and Mark Mascal *[a]

Received 21st August 2021,
Accepted 27th October 2021

DOI: 10.1039/d1tc03951b

rsc.li/materials-c

p-Type molecular dopants are a class of high electron affinity (EA) molecules used to ionize organic electronic materials for device applications. It is extremely challenging to ionize high-performance, high-ionization energy (IE) polymers because the dopant molecule needs to be compatible with solution processing. Here, we describe the synthesis and characterization of two new solution processable molecular dopants with the highest EA values yet reported. These molecules, based on the parent hexacyanotrimethylenecyclopropane (CN6-CP) structure, achieve solubility by the substitution of one or more of the cyano groups with esters, which both reduces the volatility relative to CN6-CP and allows for solution processing. The efficacy of these new molecular dopants, which have EA values up to 5.75 eV with respect to vacuum, was tested by performing sequential solution doping experiments with a series of thiophene and alternating diketopyrrolopyrrole polymers with IEs ranging from 5.10 eV to 5.63 eV. For completeness, the new dopant results are compared to a previously reported tri-ester substituted CN6-CP analogue with an EA of 5.50 EV. The increased EA of these stronger dopants induces a 10–100 fold increase in film conductivity and saturation of the conductivity at 15–100 S cm^{-1} for almost all polymers tested. These new dopant structures enable controlled solution doping at high doping levels for most alternating co-polymers of interest to the organic electronics community.

Introduction

Essentially all modern electronic devices include a combination of capacitive, resistive, emissive, and inductive components, and many incorporate power elements like batteries, photovoltaics, and thermoelectrics. Currently, these device constituents are for the most part made using inorganic materials. Recent research however has favored the use of organic polymers for opto-electronic applications due to their advanced materials properties that include light weight, flexibility, chemical tunability, and superior absorption/emission properties. Organic semiconductors (OSCs) are generally combined with molecular dopants to increase conductivity or fill trap sites.[1] Molecular dopants are small molecules with a reduction/oxidation potential sufficient to ionize sites on OSCs for p-/n-type doping, respectively. Organic semiconductors based on the poly(2,5-bis(3-alkyl-2-thienyl) thieno[3,2-*b*]thiophene) (PBTTT) framework have, for example, been reported to achieve conductivities >1000 S cm^{-1} using a variety of molecular dopants.[2–4]

p-Type OSCs have ionization energies (IE) that range from about 4.0 to 5.8 eV w.r.t vacuum. It is especially difficult to achieve high doping levels in polymers with IE greater than 5.3 eV because few dopants have sufficient electron affinity (EA) to ionize them. In particular, the high ionization energies of alternating push–pull co-polymers used for high-performance organic photovoltaic and transistor devices make efficient doping a major challenge for this class of materials.[1,5] Also, depending on the relative positions of the energy levels, molecular geometry, temperature, and carrier solvent, the same dopant could induce a molecular charge transfer (CT) state, a polaron, or a bipolaron.[6–10] Coupled to this are the limited options for solution processable dopants with high EA. This limitation comes because high EA molecules are highly reactive and thereby unstable in the presence of H_2O and most organic solvents. The dopant molecule also needs to have a stable anionic form that does not cause side reactions in the polymer film.

[a] Department of Chemistry, University of California Davis, Davis, CA, 95616, USA. E-mail: mjmascal@ucdavis.edu
[b] Department of Chemical Engineering, University of California Davis, CA, 95616, USA

† Electronic supplementary information (ESI) available. See DOI: 10.1039/d1tc03951b

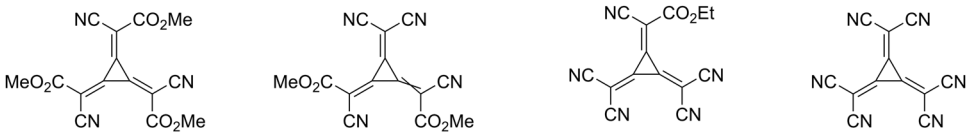

Fig. 1 Structures of trimethylenecyclopropane-based dopants **TMCN3-CP**, **DMCN4-CP**, **ECN5-CP**, and **CN6-CP** in order of increasing EA.

The p-type molecular dopant with highest EA reported to the date is 2,2′,2″-(cyclopropane-1,2,3-triylidene)trimalononitrile, or **CN6-CP**, with an EA of 5.87 eV.[11] Doping with **CN6-CP** has been demonstrated using thermal evaporation and *via* chemical deposition,[12] however, due to extreme reactivity and low solubility, it is very difficult to process *via* solution. Also, **CN6-CP** sublimes at <200 °C, making the dopant molecule itself difficult to handle.[13] Recently, we described the preparation of trimethyl 2,2′,2″-(cyclopropane-1,2,3-triylidene)tris(cyanoacetate) or **TMCN3-CP**, an analogue of **CN6-CP** in which three of the six nitrile groups were replaced with methyl esters.[14] This derivatization greatly increased the solution processability and reduced the volatility of the dopant, with a marginal penalty in EA (5.50 eV). It was shown that high ionization energy alternating copolymers such as pDPP-4T, pDPP-3T, and pDPP-T-TT-T could be p-type doped with **TMCN3-CP** to achieve high conductivities using sequential solution processing.

Here, we describe the synthesis of the corresponding dimethyl ester (**DMCN4-CP**) and monoethyl ester (**ECN5-CP**) analogues of **CN6-CP** (Fig. 1), which were predicted to be stronger dopants than **TMCN3-CP** and thus approach the highest EA achievable for organic-soluble dopants, and with which we report the sequential solution doping[15] of a series of structurally similar conjugated polymers with increasing ionization energies. We demonstrate high conductivity of 15–100 S cm^{-1} for several polymers with IE above 5.3 eV and saturation of the conductivity with increased dopant concentration, which indicates that the conductivity is no longer limited by the doping level, but instead by morphological factors.

Results and discussion

Synthesis of DMCN4-CP and ECN5-CP dopants

TMCN3-CP, the trimethyl ester analogue of **CN6-CP**, had been prepared using a modification of the method of Karpov *et al.*[13] for the synthesis of **CN6-CP** from tetrachlorocyclopropene **1** by simply substituting malononitrile for methyl cyanoacetate.[14] The synthesis of the corresponding diester and monoester analogues however presented a more significant challenge. Starting from a method for sequential substitution of tetrachlorocyclopropene **1** reported by Fukunaga,[16] treatment with methyl cyanoacetate in the presence of excess triethylamine gave zwitterion **2** (Scheme 1). Substitution of the ammonium group with malononitrile as shown gave the bis(tetrabutylammonium) salt of **DMCN4-CP**$^{2-}$ which, after counterion exchange with sodium, was oxidized with persulfate to the stable radical anion salt K$^+$ **DMCN4-CP**$^{\bullet-}$. The final oxidation with nitrosonium tetrafluoroborate proved more challenging than in the synthesis of **TMCN3-CP** and could only be effected using an excess of the oxidant at a concentration of the radical anion precursor no higher than 0.01 M. The isolated bright yellow product was identified by NMR as an inseparable 1 : 2 mixture of the *E,E* and *E,Z* stereoisomers of **DMCN4-CP.** The electron affinity of the **DMCN4-CP** stereomixture was 5.61 eV as inferred from

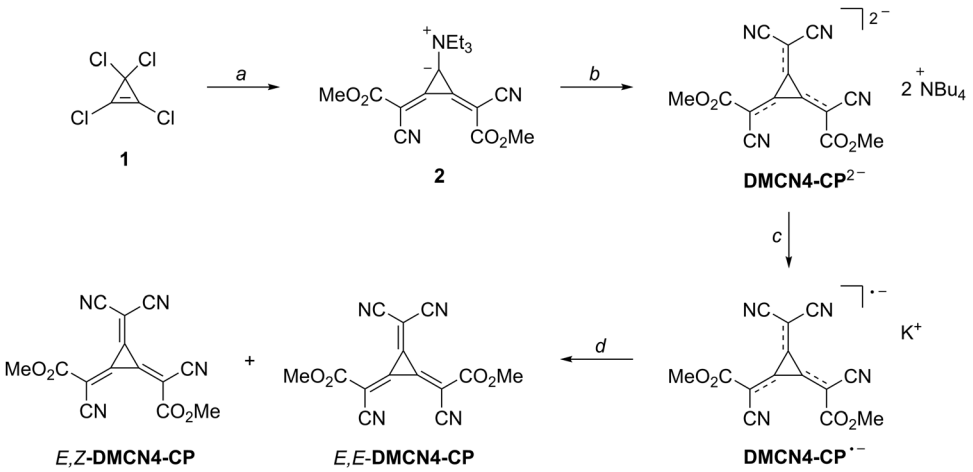

Scheme 1 Synthesis of the **DMCN4-CP** dopant. Reagents and conditions: (a) MeO_2CCH_2CN, NEt_3, CH_2Cl_2, 96%; (b) $NCCH_2CN$, NaOMe, MeOH–HMPA, Bu_4NBr, 58%; (c) NaI, MeCN; then $K_2S_2O_8$, H_2O, 72%; (d) $NOBF_4$, CH_2Cl_2, 70%.

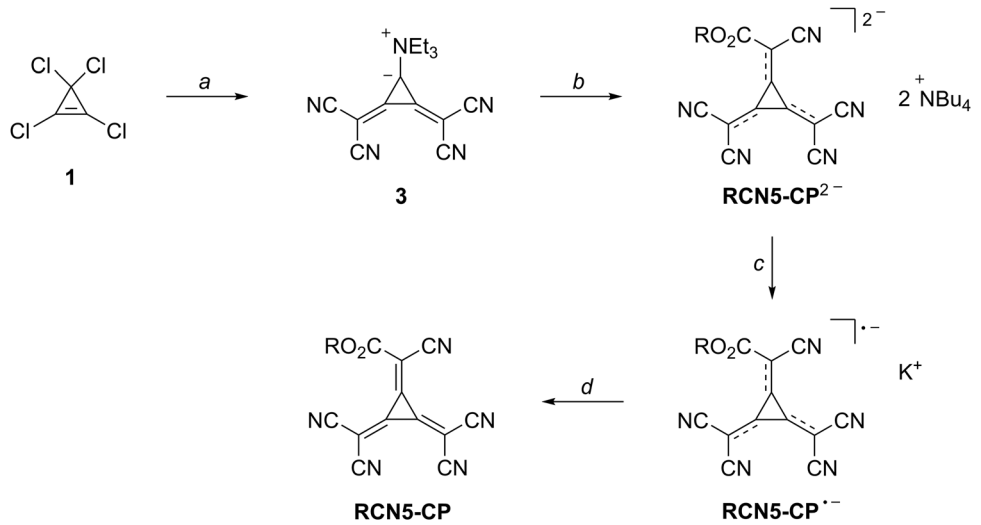

Scheme 2 Synthesis of **RCN5-CP** dopants. Reagents and conditions: (a) $NCCH_2CN$, NEt_3, CH_2Cl_2, 92%; (b) RO_2CCH_2CN, NaOMe, MeOH–HMPA, Bu_4NBr, 93% (R = M), 87% (R = E); (c) NaI, MeCN; then $K_2S_2O_8$, H_2O, 74% (R = M), 63% (R = E); (d) $NOBF_4$, CH_2Cl_2/TFA, 41% (R = E).

measurement of the reduction potential by cyclic voltammetry (CV), a significant increase over **TMCN3-CP** (5.50 eV).

The approach to the pentacyanomonoester analogue paralleled the above synthetic route but the substitution order was reversed, with malononitrile added first to **1** followed by methyl cyanoacetate, leading from **3** to the monomethyl ester dianion **RCN5-CP**$^{2-}$ and from there to radical anion salt K^+ **RCN5-CP**$^{\bullet-}$, where R = methyl (M) (Scheme 2). Although treatment of this radical anion with $NOBF_4$ led to the signature color change from blue to bright yellow, the product **MCN5-CP** proved too reactive to isolate. Changing the ester alkyl group from methyl to ethyl (E) and including TFA in the final oxidation step overcame this issue, and corresponding monoethyl ester dopant **RCN5-CP**, where R = E, could be isolated as a bright yellow powder. The electron affinity of **ECN5-CP** was 5.75 eV, as inferred from measurement of the reduction potential by CV, the highest EA for a solution-processible neutral molecular dopant to date.

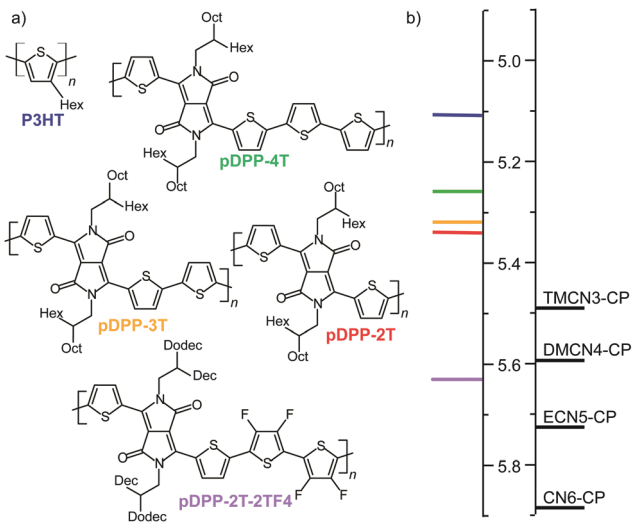

Fig. 2 Molecular structure of the polymers used in this study (a) with the ionization potential of the polymer and (b) the electron affinity of the dopant. Redox potentials were measured using CV and referenced to an energy scale.

Doping studies using DMCN4-CP and ECN5-CP

In order to test the efficacy of these new molecular dopants, we doped a series of thiophene-containing polymers which included diketopyrrolopyrrole (DPP) groups that tuned the IE range from 5.1 eV for P3HT to 5.63 eV for pDPP-2T-2TF4.[17,18] The IE of the polymers was estimated from measurement of the cyclic voltammogram in solution. It has been shown that IEs estimated in this way are generally predictive of the ionization efficiency in OSC films.[19] Fig. 2 gives the molecular structure of the five polymers investigated along with an energy level diagram that shows the ionization energies of the polymers relative to the electron affinities of the dopants.

The conductivity and thermoelectric power factor can both be maximized using the fabrication technique of sequential doping.[15,20,21] In sequential doping, the OSC layer is first coated onto the substrate and then, in a subsequent processing step, the dopant is added to the film using either evaporation[22,23] or an orthogonal solvent solution.[15,24] In this study, all OSC films were coated from 1,2-dichlorobenzene followed by sequential doping using a solution of the dopant in degassed anhydrous acetonitrile. While all strong molecular dopants react with H_2O, **ECN5-CP** and **DMCN4-CP** are also deactivated by aromatic solvents, and even trace solvent atmosphere in the glovebox can penetrate the film and dedope the polymer.[25,26]

Fig. 3 shows UV-vis-NIR spectra of each of the neat polymers and also the highest doping level reached for the **ECN5-CP** dopant. The dopant concentration was 1.0 mg mL^{-1} for each film except for pDPP-2T which was doped at 0.6 mg mL^{-1}. The pDPP-2T films became unstable with higher concentration doping and either thinned through dissolution or dewetted from

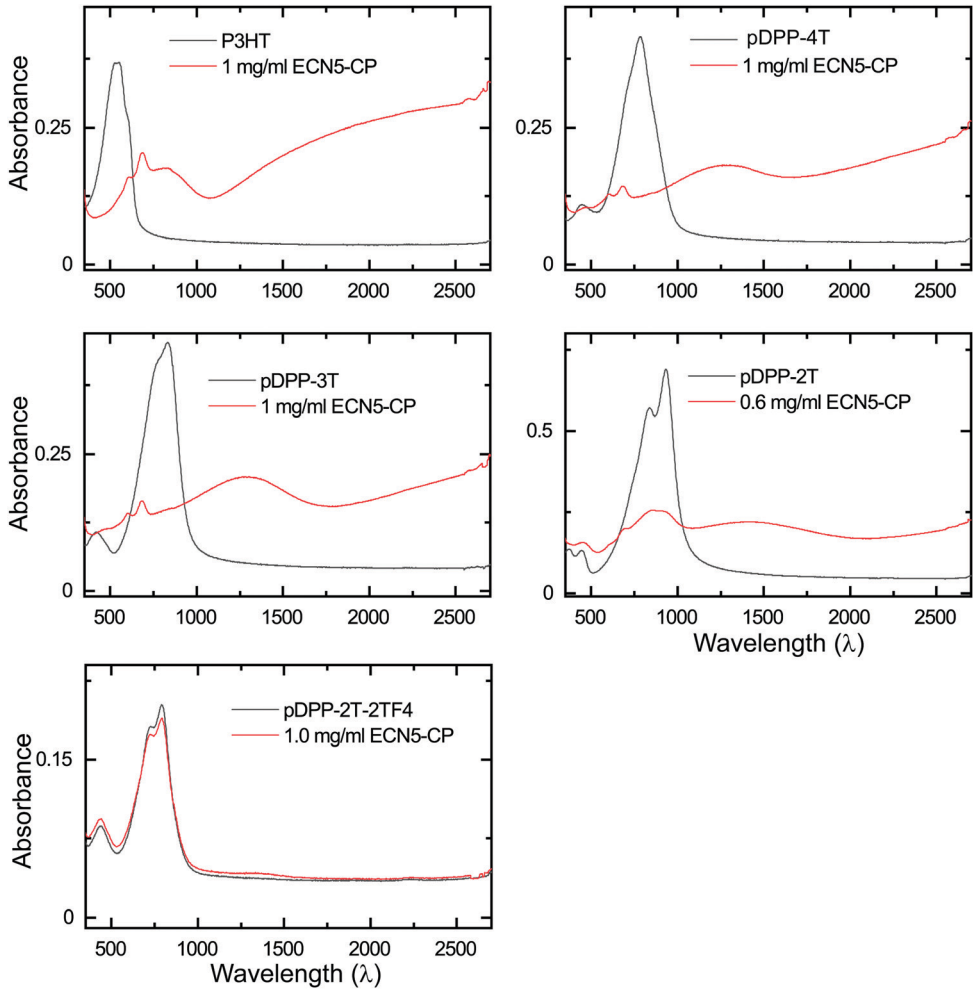

Fig. 3 UV-vis-NIR spectra of the neat polymer films (black) and an identically thick film sequentially doped with 1 mg mL^{-1} solutions of the **ECN5-CP** dopant (red) except the pDPP-2T film, which was doped with a 0.6 mg mL^{-1} solution of **ECN5-CP**.

the glass substrate. We suggest that a higher M_W polymer sample with lower PDI would be more stable during sequential doping, as has been reported previously.[27,28] In every case, the **ECN5-CP** dopant led to an integer charge transfer as can be seen from analysis of the doped spectra. With increased doping level, the neutral peaks (black lines) are bleached while at the same time polaron absorbance is detected in the NIR.[9,29] All samples also show absorbance at 595 nm and 680 nm that is attributed to the dopant anion, while no evidence of a neutral dopant absorbance is detected. In contrast, pDPP-2T-2TF4 showed almost no bleaching or polaron development, presumably because even **ECN5-CP** does not have sufficient EA to ionize this polymer.

Finally, Fig. 4 shows the four-point probe conductivity (σ) measurements for the polymers and dopants in this study plotted as a function of the doping solution concentration. We did not align the films or perform any pre- or post-processing to enhance morphology or materials properties. Each sample was simply measured directly after the solvent was evaporated from the film. The pDPP-2T-2T4F polymer is not shown because its σ was too low to detect at all doping levels. All of the other polymer samples achieved $\sigma > 15$ S cm^{-1}

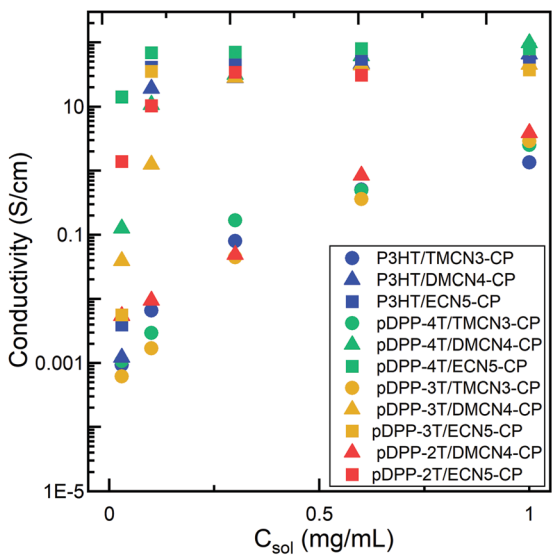

Fig. 4 Measured four-point probe conductivity *vs* doping solution concentration for polymers and dopants except for the pDPP-2T-2TF4 polymer, which did not register conductivity high enough for detection at any doping concentration.

with the **ECN5-CP** dopant and all but pDPP-2T also had $\sigma > 15$ S cm^{-1} with the **DMCN4-CP** dopant. Interestingly, pDPP-2T/**DMCN4-CP** shows almost identical σ as a function of doping solution concentration (C_{sol}) as pDPP-3T and pDPP-4T doped with the **TMCN3-CP** dopant. This indicates that there is a predictable trend with increased doping level and the dopant driving force. Finally, all four polymers reached a plateau in σ with increased C_{sol} for the **ECN5-CP** dopant, where further increasing the concentration of dopant in the solution did not result in increased conductivity. This saturation in σ was reached at C_{sol} of 0.1–0.3 mg mL^{-1}, indicating that doping equilibrium strongly favored integer charge transfer formation.

For P3HT, we observe here a maximum conductivity of ~80 S cm^{-1}, which is high, but not a record. We previously achieved 140 S cm^{-1} using anion exchange doping,[30] and Jacobs *et. al.* have reported over 200 S cm^{-1}.[3] However, most reports of high conductivity in P3HT involve directional conductivity on a doped and aligned film.[4,20,31] Thus while the result for P3HT in this work does not improve upon the conductivity reported for $FeCl_3$ doping or in aligned films, it represents the second highest conductivity achieved using a molecular dopant in an unaligned film.

Conclusions

In summary, we describe here the preparation and doping performance of two new p-type molecular dopants with record high electron affinity for organic electronics applications. Synthetically, the method used to make hexcyanotrimethylenecyclopropane **CN6-CP** was adapted to incorporate two ester groups (**DMCN4-CP**) or a single ester group (**ECN5-CP**) in the place of cyano groups. These dopants were specifically designed to be solution processable and were used for doping the semiconducting polymers P3HT, pDPP-4T, pDPP-3T, pDPP-2T and pDPP-2T-2TF4. Comparison of the dopants shows increasing ionization of polymer sites with increasing dopant strength and dopant concentration. The strongest dopant, **ECN5-CP** reached a saturation in conductivity with increased dopant concentration for all polymers except pDPP-2T-2T4F. The saturation of conductivity shows that the performance of the OSCs is not limited by hole density but can improve with changes in the polymer morphology. The molecular dopant design strategy demonstrated here provides the ability to dope high ionization energy co-polymers to high doping levels, which has been a longstanding challenge in materials science. Importantly, substitution of cyano groups for solubilizing groups enables solution processability. While we chose to substitute the cyano groups of the **CN6-CP** system with simple esters, the design strategy enables chemical tailoring to a variety of other target solubilizing groups and thus is a flexible and robust approach to improved organic electronic materials.

Methods

Optical spectroscopy

UV-vis-NIR spectra for neat films, doped films, and dopant solutions were collected using a PerkinElmer LAMBDA 750 UV/Vis/NIR spectrophotometer. The glass substrates were cleaned sequentially in ultrasonic baths of acetone, methanol, 2-propanol and deionized water. Then substrates were dried by nitrogen gun and exposed to UV/ozone for 30 min. pDPP-4T (3 mg mL^{-1}), pDPP-2T-2TF4 (3 mg mL^{-1}), pDPP-3T (5 mg mL^{-1}), and pDPP-2T (5 mg mL^{-1}) were dissolved in 1 : 1 volumetric mixture of chlorobenzene (CB) and chloroform. P3HT was dissolved in CB at a concentration of 10 mg mL^{-1}. All polymer films were spin-coated for a film thickness of ~50 nm. The thickness of the polymer films was measured with a Veeco Dektak 150 surface profilometer. For all samples, dopants were dissolved in a mixture of dichloromethane (DCM) and acetonitrile (ACN), except for pDPP-3T films doped at 1 mg mL^{-1} and 0.6 mg mL^{-1}, where only ACN was used. A separate dopant solution for each film was prepared in nitrogen glovebox (O_2 < 1 ppm, H_2O < 1 ppm) in vials that were previously baked in a vacuum oven (100 °C, 0.03 bar) overnight. Each doping solution was used as soon as prepared. The dopant solution was coated onto the polymer films and the spin coater was started to disperse the doping solution through the film. After drying, UV-vis-NIR spectra were collected under ambient conditions except for time-dependent UV-vis-NIR experiments. For time dependent experiments, the films were encapsulated in the glovebox under nitrogen (O_2 < 5 ppm, H_2O < 1 ppm) using a sample holder which was designed by the Moulé Group.

Four-probe electrical conductivity

For conductivity measurements, four electrodes (5 nm Cr/95 nm Au, 1 × 5 mm^2, 1 mm spacing) were prepared by photo-lithography using a CHA E-beam evaporator on Si with a 300 nm dielectric layer (SiO_2) in a Class 100 clean room. Si substrates were cleaned using the same procedure as described earlier for the glass substrates. Four point probe conductivity measurements were conducted using Keithley 2450 Sourcemeter. All of the conductivity measurements were carried out in the dark under nitrogen in a glovebox (O_2 < 5 ppm, H_2O < 5 ppm).

Dopant stability measurements

In order to determine the stability of doped films, a lifetime analysis using the UV-vis-NIR data was performed. We simply measured the same sample repeatedly in air whether the samples were stored in air or N_2.

Fig. S1 in the ESI† shows the UV/vis/NIR spectra taken as a function of time. Clearly the polaron peaks bleach with time while the neutral absorbance increases. The features at 2.5–3 eV are neutral dopant, which are gone with the first 15 min. This shows the very high sensitivity of the neutral dopants to trace solvent molecules. The ionized dopant is much more robust.

Fig. S2 in the ESI† shows the percentage change in absorbance for the polaron in a P3HT/**ECN5-CP** sample in air vs stored in N_2. The dopant has poor stability in general, but good data can be taken if the sample is measured immediately. Any exposure to air leads to rapid degradation of the polaron density.

Dopant synthesis

2,3-Bis(1-cyano-2-methoxy-2-oxoethylidene)-1-(triethylammonio) cyclopropan-1-ide (2). To a solution of tetrachlorocyclopropene **1** (0.37 mL, 0.54 g, 3.0 mmol) and methyl cyanoacetate (0.56 mL, 0.63 g, 6.3 mmol) in anhydrous CH_2Cl_2 (15 mL) at −30 °C was added triethylamine (2.59 mL, 1.88 g, 18.6 mmol) and the stirred mixture was allowed to come to 0 °C over 2 h. CH_2Cl_2 was added until all solids dissolved (about 20 mL). The reaction mixture was washed with water (3 × 30 mL), dried ($MgSO_4$), and concentrated under reduced pressure. The residue was suspended in Et_2O (50 mL) and the mixture was filtered and washed with fresh Et_2O (50 mL) to give **2** as an inseparable *ca.* 2.5 : 1 mixture of *E*,*Z* and *E*,*E* stereoisomers (951 mg, 96%) as an off-white powder. ^{1}H NMR (400 MHz, $CDCl_3$) δ *E*,*Z* isomer (*ca.* 70%) 4.05 (q, J = 7.2 Hz, 6H), 3.83 (s, 3H), 3.76 (s, 3H, overlapping with signal from *E*,*E* isomer), 1.41–1.29 (m, 9H, overlapping with signal from *E*,*E* isomer); *E*,*E* isomer (*ca.* 30%) 4.14 (q, J = 7.2 Hz, 6H), 3.73 (s, 6H, overlapping with signal from *E*,*Z* isomer), 1.41–1.29 (m, 9H, overlapping with signal from *E*,*Z* isomer); ^{13}C NMR (101 MHz, $CDCl_3$) δ 168.0, 165.7, 134.6, 134.2, 133.3, 120.8, 118.2, 118.1, 112.8, 111.8, 59.4, 58.7, 58.0, 57.4, 52.0, 51.8, 51.8, 46.2, 8.7, 8.6; HRMS (ESI^+) $C_{17}H_{22}N_3O^+$ $[M + H]^+$ m/z calcd 332.1599, found 332.1602.

Potassium dimethyl 2,2′-(3-(dicyanomethylene)cyclopropane-1,2-diylidene)-bis(2- cyanoacetate) radical anion salt (K^+ DMCN4-CP$^{\bullet-}$). To a solution of malononitrile (405 mg, 6.14 mmol) in MeOH (20 mL) was added NaOMe (5.4 M solution in MeOH, 1.14 mL, 6.1 mmol). The reaction mixture was stirred at rt for 30 min then cooled to 0 °C. A solution of **2** (885 mg, 2.67 mmol) in HMPA (25 mL) was added and the stirred mixture was allowed to warm up to rt over 30 min. After a further 2.5 h tetrabutylammonium bromide (4.30 g, 13.4 mmol) was added. The volatiles were removed under reduced pressure and the residue was diluted with water (200 mL). The precipitated $(NBu_4^+)_2$**DMCN4-CP**$^{2-}$ was collected by filtration, washed with water (100 mL), air dried, and used directly without further purification. This material was dissolved in acetonitrile (7.5 mL) and sodium iodide (693 mg, 4.62 mmol) was added. The mixture was stirred at rt for 30 min. The resulting Na_2**DMCN4-CP**$^{2-}$ was collected by filtration, washed with acetonitrile (25 mL), air dried, and used directly without further purification. This material was added in a single portion to a solution of potassium persulfate (596 mg, 2.20 mmol) in water (15 mL) and the reaction was stirred at rt for 1 h. Brine (50 mL) was added and the resulting precipitate was collected by filtration. The crude product was dissolved in acetonitrile (100 mL), the solution was filtered, and the solvent was evaporated under reduced pressure to give K^+**DMCN4-CP**$^{\bullet-}$ (360 mg, 42% over 3 steps) as a purple powder. HRMS (ESI^-) $C_{14}H_6N_4O_4^-$ $[M]^-$ m/z calcd 294.0395, found 294.0387; mp 238 °C (decomp.). NMR spectra of this product could not be obtained due to its open shell nature.

Dimethyl 2,2′-(3-(dicyanomethylene)cyclopropane-1,2-diylidene) (2*Z*,2′*E*)-bis(2-cyanoacetate) (*E*,*Z*-DMCN4-CP) and dimethyl 2,2′-(3-(dicyanomethylene)cyclopropane-1,2-diylidene)(2E,2′*E*)-bis(2-cyanoacetate) (*E*,*E*-DMCN4-CP). All operations were performed in a glovebox under a dry nitrogen atmosphere. To a suspension of K^+ **DMCN4-CP**$^{\bullet-}$ (142 mg, 0.426 mmol) in anhydrous CH_2Cl_2 (30 mL) was added $NOBF_4$ (498 mg, 4.26 mmol) and the mixture was stirred at rt for 30 min. The solids were removed by filtration and the filtrate was diluted with a mixture of *n*-hexane (250 mL) and TFA (1.0 mL). The resulting yellow precipitate was collected by filtration and dried in a stream of dry nitrogen for 3 h to give **DMCN4-CP** as a yellow powder which was an inseparable *ca.* 2 : 1 mixture of *E*,*Z* and *E*,*E* stereoisomers (88.0 mg, 70%). ^{1}H NMR ($CDCl_3$) δ *E*,*E* isomer (*ca.* 33%) 4.09 (s, 6H, overlapping with signal from minor isomer); *E*,*Z* isomer (*ca.* 67%) 4.09 (s, 3H, overlapping with signal from major isomer), 4.07 (s, 3H, overlapping with signal from major isomer). No ^{13}C NMR data were collected due to insufficient solubility of the compound in inert deuterated solvents.

2,3-Bis(dicyanomethylene)-1-(triethylammonio)cyclopropan-1-ide (3). To a solution of tetrachlorocyclopropene **1** (0.37 mL, 0.54 g, 3.0 mmol) and malononitrile (416 mg, 6.30 mmol) in anhydrous CH_2Cl_2 (15 mL) at −30 °C was added triethylamine (2.59 mL, 1.88 g, 18.6 mmol) and the stirred mixture was allowed to come to 0 °C over 2 h. The reaction was diluted with water (10 mL) and the precipitate was collected by filtration and washed with water (50 mL) and Et_2O (50 mL) to give **3** (732 mg, 92%) as an off-white solid. ^{1}H NMR (400 MHz, CD_3CN) δ 3.73 (q, J = 7.2 Hz, 6H), 1.34 (t, J = 7.2 Hz, 9H); ^{13}C NMR (101 MHz, CD_3CN) δ 136.7, 117.6, 116.8, 113.4, 59.6, 36.7, 9.0; HRMS (ESI^+) $C_{15}H_5N^+$ $[M + H]^+$ m/z calcd 266.1394, found 266.1390.

Potassium methyl 2-(2,3-bis(dicyanomethylene)cyclopropylidene)-2-cyanoacetate radical anion (K^+ MCN5-CP$^{\bullet-}$). To a solution of methyl cyanoacetate (0.54 mL, 0.61 g, 6.1 mmol) in MeOH (20 mL) was added NaOMe (5.4 M solution in MeOH, 1.12 mL, 6.1 mmol). The reaction mixture was stirred at rt for 30 min then cooled to 0 °C. A solution of **3** (700 mg, 2.64 mmol) in HMPA (25 mL) was added with stirring. The mixture was allowed to warm to rt over 30 min and stirred a further 2.5 h. Tetrabutylammonium bromide (4.26 g, 13.2 mmol) was added and the volatiles were removed under reduced pressure. The residue was diluted with water (200 mL) and the precipitated $(NBu_4^+)_2$**MCN5-CP**$^{2-}$ was collected by filtration, washed with water (100 mL), air dried, and used directly without further purification. This material was dissolved in acetonitrile (10 mL) and sodium iodide (1.00 g, 6.69 mmol) was added. The mixture was stirred at rt for 30 min. The resulting Na_2**MCN5-CP**$^{2-}$ was collected by filtration, washed with acetonitrile (50 mL), air dried, and used directly without further purification. This material was added in a single portion to a solution of potassium persulfate (792 mg, 2.93 mmol) in water (20 mL) and the reaction mixture was stirred at rt for 1 h. Brine (50 mL) was added and the resulting precipitate was collected by filtration. The crude product was dissolved in acetonitrile (100 mL), the solution was filtered, and the solvent was evaporated under reduced pressure to give K^+ **MCN5-CP**$^{\bullet-}$ (474 mg, 69% over 3 steps) as a purple powder. HRMS (ESI) $C_{13}H_3N_5O_2^-$ $[M]^-$ m/z calcd 261.0292, found 261.0289; mp 231 °C (decomp). NMR spectra of this product could not be obtained due to its open shell nature.

Potassium ethyl 2-(2,3-bis(dicyanomethylene)cyclopropylidene)-2-cyanoacetate radical anion (K^+ ECN5-CP$^{\bullet-}$). To a solution of ethyl

cyanoacetate (0.22 mL, 0.23 g, 2.1 mmol) in MeOH (7 mL) was added NaOMe (110 mg, 2.04 mmol). The reaction mixture was stirred at rt for 30 min then cooled to 0 °C. A solution of **3** (235 mg, 0.886 mmol) in HMPA (9 mL) was added with stirring. The mixture was allowed to warm to rt over 30 min and stirred a further 2.5 h. Tetrabutylammonium bromide (1.43 g, 4.43 mmol) was added and the volatiles were removed under reduced pressure. The residue was diluted with water (100 mL) and the precipitated $(NBu_4^+)_2$**ECN5-CP**$^{2-}$ was collected by filtration, washed with water (50 mL), air dried, and used directly without further purification. This material was dissolved in acetonitrile (4 mL) and sodium iodide (344 mg, 2.30 mmol) was added. The mixture was stirred at rt for 30 min. The resulting Na_2**ECN5-CP**$^{2-}$ was collected by filtration, washed with acetonitrile (10.0 mL), air dried and used directly without further purification. This material was added in a single portion to a solution of potassium persulfate (206 mg, 0.761 mmol) in water (2.5 mL) and the reaction mixture was stirred at rt for 1 h. Brine (10 mL) was added and the resulting precipitate was collected by filtration. The crude product was dissolved in acetonitrile (25 mL), the solution was filtered, and the solvent was evaporated under reduced pressure to give K^+ **ECN5-CP**$^{\bullet -}$ (167 mg, 54% over 3 steps) as a purple powder. HRMS (ESI) $C_{14}H_5N_5O_2^-$ $[M]^-$ *m*/*z* calcd 275.0449, found 275.0439; mp 233 °C (decomp). NMR spectra of this product could not be obtained due to its open shell nature.

Ethyl 2-(2,3-bis(dicyanomethylene)cyclopropylidene)-2-cyanoacetate (ECN5-CP). All operations were performed in a glovebox under a dry nitrogen atmosphere. To a suspension of K^+ **ECN5-CP**$^{\bullet -}$ (120 mg, 0.379 mmol) in anhydrous 15 : 1 CH_2Cl_2/TFA (30 mL) was added $NOBF_4$ (443 mg, 3.79 mmol) and the mixture was stirred at rt for 30 min. The solids were removed by filtration and the filtrate was diluted *n*-hexane (150 mL). The resulting yellow precipitate was collected by filtration and dried in a stream of nitrogen for 3 h to give **ECN5-CP** (43.0 mg, 41%) as a yellow powder. No NMR data were collected due to the high reactivity of the compound in deuterated solvents.

Conflicts of interest

There are no conflicts to declare.

References

1 B. Lüssem, C.-M. Keum, D. Kasemann, B. Naab, Z. Bao and K. Leo, *Chem. Rev.*, 2016, **116**, 13714–13751.

2 C. Y. Kao, B. Lee, L. S. Wielunski, M. Heeney, I. McCulloch, E. Garfunkel, L. C. Feldman and V. Podzorov, *Adv. Funct. Mater.*, 2009, **19**, 1906–1911.

3 I. E. Jacobs, Y. Lin, Y. Huang, X. Ren, D. Simatos, C. Chen, D. Tjhe, M. Statz, L. Lai, P. A. Finn, W. G. Neal, G. D'Avino, V. Lemaur, S. Fratini, D. Beljonne, J. Strzalka, C. B. Nielsen, S. Barlow, S. R. Marder, I. McCulloch and H. Sirringhaus, *Adv. Mater.*, 2021, 2102988, DOI: 10.1002/adma.202102988.

4 V. Vijayakumar, Y. H. Zhong, V. Untilova, M. Bahri, L. Herrmann, L. Biniek, N. Leclerc and M. Brinkmann, *Adv. Energy Mater.*, 2019, **9**, 1900266.

5 A. F. Paterson, S. Singh, K. J. Fallon, T. Hodsden, Y. Han, B. C. Schroeder, H. Bronstein, M. Heeney, I. McCulloch and T. D. Anthopoulos, *Adv. Mater.*, 2018, **30**, e1801079.

6 D. A. Stanfield, Y. Wu, S. H. Tolbert and B. J. Schwartz, *Chem. Mater.*, 2021, **33**, 2343–2356.

7 M. G. Voss, J. R. Challa, D. T. Scholes, P. Y. Yee, E. C. Wu, X. Liu, S. J. Park, O. León Ruiz, S. Subramaniyan, M. Chen, S. A. Jenekhe, X. Wang, S. H. Tolbert and B. J. Schwartz, *Adv. Mater.*, 2021, **33**, 2000228.

8 E. M. Thomas, K. A. Peterson, A. H. Balzer, D. Rawlings, N. Stingelin, R. A. Segalman and M. L. Chabinyc, *Adv. Electron. Mater.*, 2020, 2000595.

9 I. Salzmann, G. Heimel, M. Oehzelt, S. Winkler and N. Koch, *Acc. Chem. Res.*, 2016, **49**, 370–378.

10 D. Kiefer, R. Kroon, A. I. Hofmann, H. D. Sun, X. J. Liu, A. Giovannitti, D. Stegerer, A. Cano, J. Hynynen, L. Yu, Y. Zhang, D. Nai, T. F. Harrelson, M. Sommer, A. J. Moulé, M. Kemerink, S. R. Marder, I. McCulloch, M. Fahlman, S. Fabiano and C. Müller, *Nat. Mater.*, 2019, **18**, 149–155.

11 (*a*) T. Fukunaga, *J. Am. Chem. Soc.*, 1976, **98**, 610–611; (*b*) T. Fukunaga, M. D. Gordon and P. J. Krusic, *J. Am. Chem. Soc.*, 1976, **98**, 611–613.

12 Y. Liu, B. Nell, K. Ortstein, Z. Wu, Y. Karpov, T. Beryozkina, S. Lenk, A. Kiriy, K. Leo and S. Reineke, *ACS Appl. Mater. Interfaces*, 2019, **11**, 11660–11666.

13 Y. Karpov, T. Erdmann, I. Raguzin, M. Al-Hussein, M. Binner, U. Lappan, M. Stamm, K. L. Gerasimov, T. Beryozkina, V. Bakulev, D. V. Anokhin, D. A. Ivanov, F. Günther, S. Gemming, G. Seifert, B. Voit, R. Di Pietro and A. Kiriy, *Adv. Mater.*, 2016, **28**, 6003–6010.

14 J. Saska, G. Gonel, Z. I. Bedolla Valdez, S. D. Aronow, A. S. Dudnik, A. J. Moulé and M. Mascal, *Chem. Mater.*, 2019, **31**, 1500–1506.

15 I. E. Jacobs, J. Li, E. W. Aasen, J. Lopez, T. Fonseca, G. Zhang, P. Stroeve, M. P. Augustine, M. Mascal and A. J. Moule, *J. Mater. Chem. C*, 2016, **4**, 3454–3466.

16 T. Fukunaga, *US Pat., 3963769A*, 1976.

17 C. B. Nielsen, M. Turbiez and I. McCulloch, *Adv. Mater.*, 2013, **25**, 1859–1880.

18 Y. Li, P. Sonar, L. Murphy and W. Hong, *Energy Environ. Sci.*, 2013, **6**, 1684–1710.

19 B. Wegner, L. Grubert, C. Dennis, A. Opitz, A. Röttger, Y. Zhang, S. Barlow, S. R. Marder, S. Hecht, K. Müllen and N. Koch, *J. Mater. Chem. C*, 2019, **7**, 13839–13848.

20 V. Untilova, J. Hynynen, A. I. Hofmann, D. Scheunemann, Y. Zhang, S. Barlow, M. Kemerink, S. R. Marder, L. Biniek, C. Muller and M. Brinkmann, *Macromolecules*, 2020, **53**, 6314–6321.

21 E. M. Thomas, B. C. Popere, H. Fang, M. L. Chabinyc and R. A. Segalman, *Chem. Mater.*, 2018, **30**, 2965–2972.

22 I. E. Jacobs, J. Li, S. L. Berg, D. J. Bilsky, B. T. Rotondo, M. P. Augustine, P. Stroeve and A. J. Moule, *ACS Nano*, 2015, **9**, 1905–1912.

23 E. Lim, K. A. Peterson, G. M. Su and M. L. Chabinyc, *Chem. Mater.*, 2018, **30**, 998–1010.
24 D. T. Scholes, S. A. Hawks, P. Y. Yee, H. Wu, J. R. Lindemuth, S. H. Tolbert and B. J. Schwartz, *J. Phys. Chem. Lett.*, 2015, **6**, 4786–4793.
25 L. Chang, H. W. A. Ladermann, J.-B. Bonekamp, K. Meerholz and A. J. Moulé, *Adv. Funct. Mater.*, 2011, **21**, 1779–1787.
26 I. E. Jacobs, F. Wang, Z. I. Bedolla Valdez, A. N. Ayala Oviedo, D. J. Bilsky and A. J. Moule, *J. Mater. Chem. C*, 2018, **6**, 219–225.
27 J. Li, D. M. Holm, S. Guda, Z. I. Bedolla-Valdez, G. Gonel, I. E. Jacobs, M. A. Dettmann, J. Saska, M. Mascal and A. J. Moule, *J. Mater. Chem. C*, 2019, **7**, 302–313.
28 Z. I. Bedolla-Valdez, R. Xiao, C. Cendra, A. S. Fergerson, Z. K. Chen, G. Gonel, A. Salleo, D. Yu and A. J. Moule, *Adv. Electron. Mater.*, 2020, **6**, 2000469.
29 R. Ghosh, C. K. Luscombe, M. Hambsch, S. C. B. Mannsfeld, A. Salleo and F. C. Spano, *Chem. Mater.*, 2019, **31**, 7033–7045.
30 T. L. Murrey, M. A. Riley, G. Gonel, D. D. Antonio, L. Filardi, N. Shevchenko, M. Mascal and A. J. Moule, *J. Phys. Chem. Lett.*, 2021, **12**, 1284–1289.
31 S. Qu, Q. Yao, L. Wang, Z. Chen, K. Xu, H. Zeng, W. Shi, T. Zhang, C. Uher and L. Chen, *NPG Asia Mater.*, 2016, **8**, e292.